Supporting Information Appendix

Hydrology and density feedbacks control the ecology of intermediate hosts of schistosomiasis across habitats in seasonal climates

Javier Perez-Saez[1], Theophile Mande[1], Natalie Ceperley[2], Lorenzo Mari[3], Enrico Bertuzzo[1], Marino Gatto[3], Andrea Rinaldo[1,4,5]

[1] Laboratory of Ecohydrology, School of Architecture, Civil and Environmental Engineering, École Polytechnique Fédérale de Lausanne,CH-1015 Lausanne (CH)
[2] Department of Civil Engineering, University of British Columbia, Vancouver, British Columbia (CA)
[3] Dipartimento di Ingegneria Elettronica, Informazione e Bioingegneria, Politecnico di Milano, 20133 Milano (IT)
[4] Dipartimento di Ingegneria Civile, Edile ed Ambientale, Università di Padova, I-35131 Padova (IT)
[5] To whom correspondence should be addressed. E-mail: andrea.rinaldo@epfl.ch

S1 Ecological and environmental data

Field sites Three villages were retained along the transition from the Sudanian to Sahelian climatic zones (Fig. S1) (see also [1]). The choice of these experimental sites accounted for the spatially varying climatic conditions in Burkina Faso, the habitat preferences of the snail intermediate hosts (Table S1), previously studied habitats (see [2, 3]), and logistic constraints (site accessibility, travel time, total available budget). The sampling sites were selected to cover the range of habitats harboring snail hosts (see Table S1), including an irrigation canal, a temporary pond, one ephemeral stream and one permanent stream. Panamasso (11°23′23.4″N, 4°12′02.5″W) is a village adjacent to a small perennial stream in the South-Western part of the country. The Lioulgou site (12°00′38.8″N, 0°21′48.2″W) lies in the central part of the country in a lowland subject to flooding (with the creation of temporary ponds) during the wet season and mostly dry to very dry during the rest of the year (Fig. S1). Finally, Tougou (13°41′06.0″N, 2°14′22.2″W) is located in the Northern Sahelian climate next to a reservoir that feeds a network of permanent irrigation canals active almost year round. In total, four sampling locations were retained in the three experimental sites, one on the perennial stream in Panamasso, two in Lioulgou in the ephemeral stream draining the low-land and in a temporary pond, and one in Tougou within an irrigation canal.

Ecological data and sampling protocol Representative host species of both urinary and intestinal parasites were sampled over 15 months in the three selected villages with distinct climatic and environmental characteristics. Snail demographic data consisted of relative abundance counts in the four sampling sites between May/July 2014 and October 2015.
A time-based snail sampling technique was employed analogously to the one previously used in malacological studies in the country [2, 4]. The sampling protocol consisted of systematically scooping the investigated habitats for 30 minutes using a 2mm metal mesh [5, 6]. The number of collected snails and sampling metadata were recorded in dedicated sampling sheets. *Bulinus* spp. or *Biomphalaria* spp. specimens were stored in dated collection cups in a mixture of clear well water and (90%) alcohol (see e.g. [4]). Sampling was undertaken by field technicians suitably trained by our campaign management. Training was provided during one week before the start of the campaign, and feedback was given by bi-weekly contacts (phone calls) and regular on-site visits during the entire sampling campaign. Biological samples were sent every 3 months back to the Microbiology and Biotechnology Laboratory of the *Institut International d'Ingenierie de l'Eau et de l'Environnement* (2iE) in Ouagadougou for recounting and species identification using standard identification keys [7, 6, 4]. The main *Bulinus* species that were collected were *B. truncatus* in the irrigation canal in Tougou and in the ephemeral stream in Lioulgou, *B. senegalensis* in the temporary pond in Lioulgou, and *B. globosus* in

the perennial stream in Panamasso. A preliminary survey was carried out along the shores of the reservoir of Tougou, during which no snails were found. Given that this type of habitat had already been covered in previous studies [2], regular snail sampling was not performed along the reservoir shores. Population abundance timeseries are shown in Fig. 1 of the main text. Note that the irrigation canal was dry from April to June, while intense rainfall events flooded the canal and the surrounding rice fields in August, making the area *de facto* inaccessible during a period of about two weeks. Because of such exceptional environmental conditions, the analysis of the snail dynamics in the canal focuses on the period up to March 2015.

Wireless sensor network A total of 15 stations with three sensors each was deployed in the four sampling locations, starting May 2014 in Tougou, June 2014 in Panamasso and July 2014 in Lioulgou (Fig. S1). The stations were equipped with sensors of key hydro-meteorological parameters including air temperature, water level, conductivity and temperature, and precipitation [8] (see Fig.1 and Table S2). Measurements were taken every 30 seconds and data were sent to a central server using the mobile phone network. Data were accessible online through a dedicated web portal (`http://climaps.com`). Additional temperature data loggers were placed in the temporary pond in Lioulgou because it was not covered by the wireless stations (Table S2).

S2 Population dynamics modeling

Density feedback detection in ecological timeseries has received considerable attention in the literature, building on a common framework of relatively simple mechanistic models for population dynamics coupled with statistical methods for discriminating among alternative feedback processes [9, 10, 11]. Here, snail population dynamics were simulated by discrete-time demographic models inclusive of extrinsic environmental forcing. Specifically, if N_t denotes the abundance of the snail population in a given habitat at sampling time t, the simplest demographic model reads

$$N_{t+1} = \lambda N_t,$$

where λ corresponds, whatever its attributes, to the finite instantaneous growth rate of the population between two sampling dates. This simple Malthusian formulation can be extended to incorporate non-linear density feedback as proposed by Ricker in the form

$$N_{t+1} = \lambda N_t e^{bN_t},$$

were b is a parameter that sets the feedback' strength [12]. On taking logarithms, the Ricker model reads:

$$\log\left(\frac{N_{t+1}}{N_t}\right) = a + bN_t, \tag{S1}$$

where log is the natural logarithm, and $a = \log\lambda$. Negative density feedback occurs for $b < 0$, i.e., decreased recruitment and/or increased death rates at high population densities. In the following we denote as a the instantaneous intrinsic population growth rate. Depending on the values of a and b, the model can produce a wide range of dynamical behaviors including steady states, limit cycles and chaos [13]. Obviously, one recovers the original Malthusian model by setting $b = 0$.

Exogenous forcing of environmental covariates, their lags, and lagged effects of abundance [14], can be accounted for as:

$$\log\left(\frac{N_{t+1}}{N_t}\right) = a + \sum_{\tau_N=0}^{r_N} b_{\tau_N} N_{t-\tau_N} + \sum_{i=1}^{m}\sum_{\tau_x=0}^{r_x} c_{i\tau_x} X^i_{t-\tau_x}, \tag{S2}$$

where: b_{τ_N} and $c_{i\tau_x}$ are respectively the weights of the lagged population abundances $N_{t-\tau_N}$, and the environmental covariate features, $X^i_{t-\tau_x}$, taken at non-negative integer time lags $\tau_N \leq r_N$ and $\tau_x \leq r_X$. Lagged covariate features were taken in all possible combinations for a given maximum number m. Lagged abundance effects were only considered one at a time or all at once. Product interactions of the type $N_{t-\tau_N} X^i_{t-\tau_x}$ were not considered.

A second class of models that incorporate density feedbacks is the Gompertz scheme [15], where the feedback is a function of the logarithm of population abundance, $\mathrm{L}_t = \log(\mathrm{N}_t)$, rather than abundance itself. The Gompertz model can be cast in the same form as eq. S2, i.e.

$$\log\left(\frac{\mathrm{N}_{t+1}}{\mathrm{N}_t}\right) = a + \sum_{\tau_{\mathrm{N}}=0}^{r_{\mathrm{N}}} b_{\tau_{\mathrm{N}}} \mathrm{L}_{t-\tau_{\mathrm{N}}} + \sum_{i=1}^{m} \sum_{\tau_{\mathrm{x}}=0}^{r_{\mathrm{x}}} c_{i\tau_{\mathrm{x}}} X^i_{t-\tau_{\mathrm{x}}}. \tag{S3}$$

Note that the logarithmic dependence of the rate of increase on abundance implies a milder density feedback process.

The modeled demographic processes were assumed to be subject to multiplicative log-normal white noise, resulting in additive Gaussian for the logarithms of the discrete rates of increase i.e.

$$y_t = \log\left(\frac{\mathrm{N}_{t+1}}{\mathrm{N}_t}\right),$$

yielding a linear regression equation

$$y_t \;=\; f(\mathbf{N}, \mathbf{X}, \boldsymbol{\theta}) + \epsilon_t,$$

where $f(\cdot)$ is the model structure used for the regression, $\mathbf{N}$ is the time vector of abundance observations, $\mathbf{X}$ is the matrix of environmental covariate features, $\boldsymbol{\theta} \in \mathcal{R}^{k\times 1}$ is the vector of true regression parameters,

$$\epsilon_t \overset{\text{iid}}{\sim} \mathcal{N}(0, \sigma^2)$$

are the regression residuals, and σ is the standard deviation of the white noise.

These demographic models were also contrasted with random walk models in the standard form:

$$y_t = \epsilon_t + f(\mathbf{X}, \boldsymbol{\theta}),$$

which was also tested against all ecological time series.

S3 Model implementation and identification

The selection of demographic models required calibration via least-square regression of all possible linear combinations of covariate features within the four modeling families described in the text (namely, random walk, Malthusian, Ricker and Gompertz). Continuous environmental covariates consisted of average and standard deviation of the measurements taken over the week preceding snail sampling dates at each site (Table S2). Precipitation data covariates consisted of cumulative sums over two different windows (2 weeks and 1 month), and of the number of precipitation events - daily precipitation higher than 20mm - during the week preceding sampling dates. A limit of $r_X = 3$ time lags on the covariates was imposed, which is equivalent to taking into account habitat environmental conditions up to 1 month preceding sampling. Furthermore the maximum number of covariate features was set to $m = 7$ in the face of the relatively limited number of ecological data points (a maximum of 66 weeks of data), and the number of resulting models to be tested. Lags in the effect of population abundance were limited to $r_N = 3$, and density feedback processes were tested either individually (therefore only one lag present for each combination of environmental covariates), or all together. For a given m, all possible combinations of parameters were tested, giving a total number of models to test equal to the sum of the number of lagged covariate combinations, $\sum_{j=0}^{m} \binom{M}{j}$, were M is the total number of available features and their lags (38 in our study), times the number of model structure types (namely, random walk, Malthusian, Gompertz and Ricker) accounting for lagged abundance covariates:

$$(2(\tau_{\mathrm{N}} + 1) + 2) \sum_{j=0}^{m} \binom{38}{j} \approx \mathcal{O}(10^7)$$

for $m = 7$. Weeks in which no snails were observed were given an abundance of 1 to be able to compute logarithms. The Gompertz and Ricker models for which the estimated intrinsic rate of increase was negative, $\hat{a} < 0$, or suggesting positive density feedback, $\hat{b}_{\tau_N} > 0$, were rejected as implausible. Indeed, to our knowledge, there is no experimental evidence of positive density feedbacks for any intermediate host species of schistosomiasis. The positive constraint on a is necessary to ensure that the modeled dynamics have a positive nontrivial equilibrium abundance [13]. Multiplicative interactions between variables were not considered. The computations were run in parallel with R (R Core Team (2015). *R: A Language and Environment for Statistical Computing*. R Foundation for Statistical Computing, Vienna, Austria) and the `foreach` package (Revolution Analytics & Weston, S. (2014). *foreach: Foreach looping construct for R*, R package version 1.4.2.) on the CASTOR cluster of the Scientific IT and Application Support Center of EPFL.

S4 Model selection and abundance predictions

Statistical tools for the detection of density feedbacks have been extensively studied, for instance through the use of hypothesis testing with bootstrapping [9], or information-theoretical methods such as the Akaike information criterion (AIC) [16]. Recently, Structural Risk Minimization (SRM) has been proposed as a viable alternative tool for ecological model selection [13]. One advantage of SRM is that it does not depend on particular assumptions about the nature of the joint probability distribution of process and measurement errors. It has been shown to yield better density feedback recognition capabilities than widely used compensated Akaike information criteria (AICc) [11, 13]. Within the SRM framework, the selection criterion corresponds to the choice of the model structure and parameter set that minimize the empirical upper bound of the true structural risk (R), given by:

$$\mathrm{R}(\boldsymbol{\theta}) \leq \mathrm{R}(\widehat{\boldsymbol{\theta}}) = \frac{1}{q} \frac{\sum_{t=1}^{q} \widehat{\epsilon}_t{}^2}{\left[1 - \sqrt{p - p\log(p) + \frac{\log(q)}{2q}}\right]_+}, \tag{S4}$$

where

$$\hat{\epsilon}_t = y_t - f(\mathbf{N}, \mathbf{X}, \hat{\boldsymbol{\theta}})$$

gives the estimated model residuals associated to the vector $\hat{\boldsymbol{\theta}} \in \mathcal{R}^{k\times 1}$ of optimal parameter estimates for a given model structure $f(\cdot)$, k is the number of parameters, q is the total number of observations, and p is an index of complexity known as the VC-dimension, conveniently equal to k/q in the case of linear models. The denominator is kept if strictly positive [13].

To assess the actual predictive ability of the models retained by the SRM criterion, we performed a leave-one-out cross-validation (LOO-CV) consisting of sequentially removing one data point, re-fitting the models to the rest of the data, and predicting the values of the ignored observation. The LOO-CV residuals, say $\widetilde{\epsilon}_t$, resulting from this process are used to assess the predictive capacity of each model based on the mean squared cross-validation error [10],

$$\mathrm{MSE}^{\mathrm{cv}} = \sum_{t=1}^{q} \widetilde{\epsilon}_t{}^2/q.$$

The $\mathrm{MSE}^{\mathrm{cv}}$ is an unbiased estimator of the true expected model MSE, thus providing a way of comparing models using $\mathrm{MSE}^{\mathrm{CV}}$ ratios. Moreover candidate models can be combined using LOO-CV to obtain an optimal average model for prediction by minimizing the weighted sum of the cross-validation residuals of the retained set of models [17], resulting in the so-called jackknife model average (JMA, see below). Given the large number of tested models, here this technique was applied to a subset of the models retained using the SRM criterion. The same modeling framework was used to validate the results with the available historical ecological data in Burkina Faso gathered from the literature [2].

Fig. S4 shows that the SRM criterion can rank the models according to their predictive power (i.e. according to the smaller values of MSE^{CV}) . Density feedback processes selected by the SRM criterion were consistent

with the ones selected with other commonly used criteria. In Fig. S5 we show results for the AICc criterion [11, 13], formulated as

$$AIC_C = 2k - 2\log\left(\frac{1}{q}\sum_{t=1}^{q}\widehat{\epsilon_t}^2\right) + \frac{2k(k+1)}{q-k-1},$$

and the Bayesian information criterion (BIC), given by

$$\text{BIC} = q\log(\frac{1}{q}\sum_{t=1}^{q}\widehat{\epsilon_t}^2) + k\log(q).$$

Note that, as opposed to the SRM criterion in eq. S4, here k is the number of parameters of the model plus 1 (including the estimation of the noise variance), q is the total number of observations, and the $\widehat{\epsilon_t}$ are the estimated residuals of the model.

The roles of density feedbacks and environmental covariates are further illustrated in terms of regression coefficients values by species and habitat in Tables S3-S7. Details on lagged density feedback and covariate occurrence in best selected models for the ecology of the snail populations are given in Fig. S6, highlighting the distinct roles of hydrologic controls across habitats and climatic regimes.

S5 Jackknife model averaging

By applying models to intermediate host abundance data we pursue two goals: model identification, to disentangle the ecological processes underpinning snail population dynamics, and evaluating the model predictive capacity in the perspective of building demographic forecasting tools. Using our model selection process we obtain a set of models with minimal structural risk that can be combined to build a predictive model that outperforms any single model candidate. Model averaging consists in assigning a weight to each model. Such weight is a function of its score in terms of an information criterion such as the Akaike Information Criterion or the Bayesian Information Criterion (see [18] for an overview on model averaging techniques). Here, specifically, we use the so-called Jackknife model averaging technique (for the derivations and properties of this technique we refer the reader to [17]). The jackknife model average (JMA) estimator is asymptotically optimal when dealing with weighted averages of linear regression estimators (with positive weights summing to 1) in terms of minimizing both the in-sample fit, and the expected true error (*sensu* [19]) which accounts for un-observed data. Furthermore the JMA method holds also for heteroscedastic errors. Finally it outperforms information-criteria-based model averages on finite-sample simulation benchmark experiments [17]. In our procedure the JMA ensues directly from the computation of the leave-one-out cross-validation (LOO-CV) mean-squared error statistic used to asses model predictive power, $\text{MSE}^{\text{cv}} = \sum_{t=1}^{q}\widetilde{\epsilon_t}/q$, where the $\widetilde{\epsilon_t}$ are the residuals of the model fit to the dataset removing the data point at time t, and evaluated at time t. In the JMA framework, we seek the weight vector $\mathbf{w}$ that minimizes the expected true error of the model average. Let $\widetilde{\boldsymbol{\epsilon}^j}$ indicate the vector of jackknife residuals for model j among N candidate models. The estimate the of expected true error is

$$CV_N(\mathbf{w}) = \frac{1}{N}\mathbf{w}^T\widetilde{\boldsymbol{\epsilon}}^T\widetilde{\boldsymbol{\epsilon}}\mathbf{w} \tag{S5}$$

where CV_n is the least-square cross-validation criterion, $\widetilde{\boldsymbol{\epsilon}}$ is the matrix composed of the N LOO-CV residual vectors $\widetilde{\boldsymbol{\epsilon}^j}$, and ^{T} indicates matrix transposition. Given the expression of the expected true error, computing the optimal weight vector $\hat{\mathbf{w}}$ to obtain the JMA reduces to solving the quadratic programming problem

$$\begin{aligned} \underset{\mathbf{w}}{\text{minimize}} \quad & CV_N(\mathbf{w}) \\ \text{subject to} \quad & \mathbf{w}^T\mathbf{1}_N = 1, \\ & \text{diag}(\mathbf{w})\mathbf{1}_N \geq \mathbf{0}_N, \end{aligned}$$

where $\mathbf{0}_N, \mathbf{1}_N$ denote $N \times 1$ vectors of 0s and 1s respectively, and $\text{diag}(\mathbf{u})$ denotes a diagonal matrix with main diagonal composed of the elements of $\mathbf{u}$. The constraints force the weights to be non-negative and to sum to 1. The optimization problem can be solved using any quadratic programming tools. The `quadprog` package in R (Weingessel, A. (2013). `quadprog`*: Functions to solve Quadratic Programming Problems.* R package version 1.5-5.) was used in our analysis.

The weights of the 500 best models for each habitat and species show that only a reduced number of models are indeed included in the JMA, and that the best SRM models did not systematically appear in the model average (Fig. S7).

S6 Historical data and results validation

To our knowledge, only two field studies have specifically focused on the population dynamics of intermediate hosts of schistosomes in Burkina Faso. Both studies were conducted in the 90's and concerned a temporary pond harboring *Bulinus senegalensis* (12°11′41″N, 2°35′58″W) and a small reservoir in the central part of the country for *Bulinus truncatus* (12°12′54″N, 2°28′36″W) [2, 3]. Ecological data consisted of fortnightly relative abundance counts using a 30-min sampling technique (see Sampling protocol in this SI).

Environmental covariates were measured locally on snail sampling dates, including water temperature, conductivity and pH. Bi-weekly cumulative precipitation was available for a location adjacent to the sampling sites. Significantly, data showed an annual cycle of snail abundance with population bursts during the rainy season in both habitats, followed by subsequent population reduction and snail aestivation in the case of the temporary pond (Fig. S8). *B. senegalensis* abundance presented a double-peak in the temporary pond, with an early peak around July at the start of the rainy season and a second one around October. On the other hand, *B. truncatus* was present in the monitored reservoir during a much longer portion of the year, with a peak of population abundance at the end of January. Poda et al. investigated the correlations between snail counts and environmental covariates, reporting as significant the negative correlation with temperature for *B. truncatus*, and a positive association with pH for *B. senegalensis*.

The modeling framework used to analyze our original field observations was also applied to the historical data available for Burkina Faso. In our study we use continuously monitored environmental signals whereas only point data (on the dates of snail sampling) were available in the historical studies, thus containing less information about the environmental conditions impacting snail development and reproduction. Interestingly, density feedbacks were consistently found by contrasting Poda's reservoir data via the SRM criterion. Most of the 100 best SRM models selected for the temporary pond, however, corresponded to the random walk model, indicating that the upper bound of the structural risk does not support any ecological modeling (Fig. S9 A). It seems likely that this result stems from the limited amount of available environmental data in the 1990-1992 time series, but no proof can be provided. Nevertheless, AICc, BIC, and LOO-CV MSE favored the Gompertz model type, i.e. a mild density feedback (Fig. S9 B). This less clear-cut model identification is speculated to be a direct consequence of the lack of continuous environmental data, specifically for the temporary pond during the dry season.

The JMA was able to satisfactorily capture the multi-annual dynamics of *Bulinus* spp. in both habitats. It may be noted that the best selected models overestimate the initial population rate of increase in the reservoir whereas the JMA adequately smooths them out (Fig. S9 C). Interestingly, a density feedback in the reservoir was found to be correlated to the snail population one month before snail sampling dates, in contrast with the feedbacks identified in the habitats studied in our field work. Models for both habitats were mainly driven by water temperature (particularly in the temporary pond), with pH, cumulative precipitation and conductivity appearing less frequently (Fig. S9 D,E). The performance of the JMA is encouraging despite the lack of continuously measured environmental data for the potential of extending our eco-hydrological approach to settings with more sparse and episodic environmental and ecological data.

S7 Upscaling of climatic and hydrological drivers

Extending the forecasting capacity of the JMA for each type of habitat to other regions of Burkina Faso could provide a valuable tool for planning the application of snail control measures and for the distribution of preventive chemotherapy and mass drug administration. Since all models rely on climatic and hydrological variables for which monitoring stations such as the ones installed in our experimental sites are not widely available in the country, we propose a list of remote-sensing data sources which could be used as substitutes to field data. Needless to say, the bias (if any) and quality of remotely-sensed data could hinder the predictive capacity of our models, but we deem them valuable nonetheless for locating the most common habitats in which snails can be found, and capturing seasonality and peaks of intermediate host population abundance. Examples of remotely sensed data that are freely accessible are given in Table S8. In a first stage these data can be used to determine the spatial distribution of habitat types on large scales based on the physical and hydrological characteristics of the country. Flow accumulation rasters derived from Digital Terrain Models (DTMs), evapo-transpiration data and multi-seasonal satellite imagery can be used to determine the location and ephemerality of waterbodies at the national scale. Furthermore, existing databases on water resources infrastructure provide the localization of man-made reservoirs and valuable information on irrigation works [20]. The development of a robust methodology to perform this task is the object of ongoing work. Snail abundance fluctuations can then be inferred by feeding spatio-temporal remotely sensed data on precipitation and air, surface and water temperature into the modeling framework developed in this study. The approach we present here has the unique feature of not only yielding the possible locations of the intermediate hosts of schistosomiasis, but also providing estimates of seasonal population fluctuations. Both of these aspects represent important insights this type of approach could give to disease surveillance-response mechanisms.

References

[1] M.V.K. Sivakumar and Gnoumou Faustin. *Agroclimatology of West Africa: Burkina Faso*. International Crops Research Institute for the Semi-Arid Tropics, Patancheru, A.P. 502 324, India, 1987. Information Bulletin no.23.

[2] J.N. Poda, B. Sellin, and L. Swadago. Dynamique des populations de *Bulinus senegalensis* Müller 1781 dans une mare temporaire située dans une zone climatique nord-soudanienne au Burkina Faso. *Revue d'Elevage et de Médecine Vétérinaire des Pays Tropicaux*, 47(4):375–378, 1994.

[3] J.N. Poda, L.L. Sawadogo, Bertrand Sellin, and S. Sanogo. Dynamique des populations de *Bulinus truncatus rohlfsi* Clessin, 1886, dans le barrage de Dyoro en zone nord soudanienne du Burkina Faso. *Agronomie Africaine*, 8(1):61–68, 1996.

[4] Susanne H Sokolow, Elizabeth Huttinger, Nicolas Jouanard, Michael H Hsieh, Kevin D Lafferty, Armand M Kuris, Gilles Riveau, Simon Senghor, Cheikh Thiam, Alassane N'Diaye, et al. Reduced transmission of human schistosomiasis after restoration of a native river prawn that preys on the snail intermediate host. *Proceedings of the National Academy of Sciences*, pages 9650–9655, 2015.

[5] N. G. Hairston, B. Hubendick, J. M. Watson, and L. J. Olivier. An evaluation of techniques used in estimating snail populations. *Bulletin of the World Health Organization*, 19(4):661–72, jan 1958.

[6] Susanne H Sokolow, Kevin D Lafferty, and Armand M Kuris. Regulation of laboratory populations of snails (biomphalaria and bulinus spp.) by river prawns, macrobrachium spp.(decapoda, palaemonidae): Implications for control of schistosomiasis. *Acta tropica*, 132:64–74, 2014.

[7] David Brown. *Freshwater Snails of Africa and their Medical Importance*. Taylor & Francis, 1980.

[8] Theophile Mande, Natalie C Ceperley, Gabriel G Katul, Scott W Tyler, Hamma Yacouba, and Marc B Parlange. Suppressed convective rainfall by agricultural expansion in southeastern Burkina Faso. *Water Resources Research*, 51(7):5521–5530, 2015.

[9] Brian Dennis and Mark L Taper. Density dependence in time series observations of natural populations: estimation and testing. *Ecological Monographs*, 64(2):205–224, 1994.

[10] Peter Turchin. *Complex Population Dynamics: a Theoretical/Empirical Synthesis*, volume 35. Princeton University Press, 2003.

[11] Barry W. Brook and Corey J. A. Bradshaw. Strength of evidence for density dependence in abundance time series of 1198 species. *Ecology*, 87(6):1445–1451, June 2006.

[12] William E Ricker. Stock and recruitment. *Journal of the Fisheries Board of Canada*, 11(5):559–623, 1954.

[13] Giorgio Corani and Marino Gatto. Structural risk minimization: A robust method for density-dependence detection and model selection. *Ecography*, 30(3):400–416, 2007.

[14] Peter Turchin. Rarity of density dependence or population regulation with lags? *Nature*, 344(6267):660–663, 1990.

[15] Sofia Gamito. Growth models and their use in ecological modelling: an application to a fish population. *Ecological Modelling*, 113(1):83–94, 1998.

[16] Jerald B Johnson and Kristian S Omland. Model selection in ecology and evolution. *Trends in Ecology & Evolution*, 19(2):101–8, February 2004.

[17] Bruce E. Hansen and Jeffrey S. Racine. Jackknife model averaging. *Journal of Econometrics*, 167(1):38–46, March 2012.

[18] Gerda Claeskens, Nils Lid Hjort, et al. *Model Selection and Model Averaging*, volume 330. Cambridge University Press Cambridge, 2008.

[19] Bradley Efron. *The Jackknife, the Bootstrap and other Resampling Plans*, volume 38. SIAM, 1982.

[20] Philippe Cecchi, Aude Meunier-Nikiema, Nicolas Moiroux, Bakary Sanou, and Francis Bougaire. Why an Atlas of Lakes and Reservoirs in Burkina Faso? Technical Report iii, Small Reservoirs Project, 2007.

[21] J.N. Poda, A. Traoré, and B. K. Sondo. L'endémie bilharzienne au Burkina Faso. *Société de Pathologie Exotique*, 97(1):47–52, 2004.

[22] Philip Leifeld. texreg: Conversion of statistical model output in R to LaTeX and HTML tables. *Journal of Statistical Software*, 55(8):1–24, 2013.

[23] Bernhard Lehner, Kristine Verdin, and Andy Jarvis. New global hydrography derived from spaceborne elevation data. *EOS, Transactions American Geophysical Union*, 89(10):93–94, 2008.

[24] George J Huffman. Estimates of root-mean-square random error for finite samples of estimated precipitation. *Journal of Applied Meteorology*, 36(9):1191–1201, 1997.

[25] J.N. Poda. *Distribution spatiale des hôtes intermediaires des schistosomes au Burkina Faso: Facteurs infulençant la dynamique des populations de* Bulinus truncatus rohlfsi (Classin, 1886) et de Bulinus sengalensis *(Muller, 1781)*. PhD thesis, Université de Ouagadougou, 1996.

Table S1: Occurrence and habitat preferences of snail intermediate host species of human schistosomes in Burkina Faso. Species relative occurrence is indicated by (**+++**) most common, (++) common, (+) rare. Qualitative habitat preference is given by (***) preferred, (**) very common, (*) recurrent, (-) rare or not observed. Symbols are our interpretation of data from 496 biotopes across the country reported by [21].

Schistosome species	**Snail species**	**Occurrence**	**Habitat preference**				
			reservoir	stream	pond	irrigation canal	lake
Schistosoma haematobium	*Bulinus truncatus*	**+++**	***	**	**	*	*
	B. senegalensis	**+++**	**	**	***	-	-
	B. globosus	++	**	***	-	*	*
	B. forskalii	++	**	**	*	-	-
	B. umbilicatus	+	*	*	-	-	-
Schistosoma mansoni	*Biomphalaria pfeifferi*	**+++**	**	***	-	*	*

Table S2: Environmental covariates at sampling locations.

		Water [a,b]			Air [c]	Precipitation [d]	
Village	Site	temperature	conductivity	depth	temperature	sum [e]	events [f]
Tougou	canal	yes	yes	yes	yes	yes	yes
	reservoir	yes	yes	yes	yes	yes	yes
Lioulgou	stream	yes[g]	-	-	yes	yes	yes
	pond	yes	-	-	yes	yes	yes
Panamasso	stream	yes	yes	yes	yes	yes	yes

[a] Measurements made in Tougou and Panamasso using Decagon Devices CDT sensor, Decagon Devices, http://www.decagon.com/en/hydrology/water-level-temperature-electrical-conductivity/ctd-10-sensor-electrical-conductivity-temperature-depth/

[b] Measurements made in Lioulgou using TidBiT v2 Temp, Onset HOBO Data Loggers, Onset Computer Corporation, http://www.onsetcomp.com/products/data-loggers/utbi-001

[c] Measurements made using Decagon Devices VP-3 sensor, Decagon Devices, http://www.decagon.com/en/canopy/canopy-environment/vp-4-humidity-barometricpressure-temperature-and-vapor-pressure-sensor/

[d] Measurements made using Davis Rain Collector, Davis Instuments, http://www.davisnet.com/weather/products/weather_product.asp?pnum=07852

[e] Cumulative sum over 2 weeks and 1 month time windows preceding snail sampling dates

[f] A rainfall event is considered to be a day with total precipitation larger than 20mm

[g] Only in 2015

	model1	model2	model3	model4	model5	model6	model7	model8
a	0.435	10.24***	8.152***	0.747	−4.654***	5.719***	1.201*	−4.862***
	(0.230)	(0.732)	(0.816)	(0.421)	(0.495)	(0.536)	(0.355)	(0.519)
L_t			−1.974***	−1.446***		−1.140***	−1.346***	
			(0.118)	(0.092)		(0.089)	(0.078)	
$L_t.lag3$	−0.394***							
	(0.051)							
N_t		−0.031***						
		(0.002)						
air.temp.sd.lag1	−0.426***							
	(0.047)							
air.temp.sd.lag2	0.475***				0.330***			0.386***
	(0.048)				(0.050)			(0.052)
air.temp.sd.lag3			0.293***					
			(0.039)					
conductivity.mean.lag1		−0.052***						
		(0.004)						
conductivity.mean.lag3	0.015***		−0.031***					
	(0.002)		(0.005)					
conductivity.sd.lag2		−0.116***						
		(0.011)						
conductivity.sd.lag3				0.024	−0.008	−0.048*	0.047**	−0.005
				(0.013)	(0.014)	(0.018)	(0.013)	(0.015)
precip.14	−0.045***	0.119***						−0.024***
	(0.002)	(0.009)						(0.003)
precip.30		−0.017***						
		(0.001)						
precip.7				−0.096***			−0.089***	0.053***
				(0.017)			(0.013)	(0.006)
precip.events.14		−3.367***	0.456***		−0.618***			
		(0.262)	(0.048)		(0.065)			
precip.events.30	0.441***				0.824***			0.845***
	(0.042)				(0.073)			(0.076)
precip.events.7	2.418***			3.598***	1.462***	0.770***	3.522***	
	(0.134)			(0.513)	(0.158)	(0.110)	(0.383)	
water.level.mean					0.007***			0.007**
					(0.001)			(0.001)
water.level.mean.lag1			0.012***	0.008***		0.008***	0.007***	
			(0.001)	(0.001)		(0.001)	(0.001)	
water.level.mean.lag2	−0.002**		−0.004***			−0.005***		
	(0.000)		(0.001)			(0.001)		
water.level.sd					0.023***			0.024***
					(0.003)			(0.003)
water.level.sd.lag2				−0.011***			−0.013***	
				(0.002)			(0.002)	
water.level.sd.lag3						0.012**		
						(0.002)		
water.temp.mean				0.106***			0.090***	
				(0.015)			(0.013)	
water.temp.mean.lag1			0.071***					
			(0.012)					
water.temp.mean.lag3		−0.191***	−0.174***			−0.114***		
		(0.016)	(0.019)			(0.017)		
water.temp.sd.lag1							−0.740*	
							(0.272)	
water.temp.sd.lag3		1.992***						
		(0.218)						
R^2	0.984	0.992	0.982	0.973	0.970	0.969	0.987	0.967
Adj. R^2	0.968	0.983	0.964	0.949	0.943	0.943	0.972	0.938
Num. obs.	17	16	17	16	16	16	16	16
MSE	0.062	0.050	0.067	0.080	0.084	0.084	0.059	0.088

$^{***}p < 0.001$, $^{**}p < 0.01$, $^{*}p < 0.05$

Table S3: Regression coefficents of the 8 best SRM-ranked models of the ecology of *Bulinus* spp. in an irrigation canal. Coefficients are color-coded for significant (p-value$<$ 0.05) positive (green) and negative (red) effects on snail abundance variantions. Standard error at 95% CI is given in bellow coefficient values (light gray, in parenthesis). Environmental covariate names are color-coded by type as in Fig. 3. Table produced using R package `texreg` [22].

	model1	model2	model3	model4	model5	model6	model7
a	4.404	5.638	**2.203*****	**2.628*****	2.105	**2.962*****	**2.579*****
	(2.662)	(3.487)	(0.541)	(0.661)	(2.500)	(0.656)	(0.555)
L_t	**−0.650*****	**−0.744*****	**−0.409*****	**−0.425*****	**−0.662*****	**−0.486*****	**−0.469*****
	(0.109)	(0.133)	(0.101)	(0.105)	(0.112)	(0.105)	(0.100)
air.temp.mean	**0.786*****	**0.737*****			**0.714*****		
	(0.184)	(0.191)			(0.188)		
air.temp.mean.lag2	**−0.405***				**−0.406***		
	(0.156)				(0.165)		
air.temp.mean.lag3		**−0.379***					
		(0.182)					
air.temp.sd			**−0.282*****			−0.184	**−0.288*****
			(0.078)			(0.091)	(0.079)
air.temp.sd.lag3	**−0.674*****	**−0.684*****		**−0.399****	**−0.573*****	−0.250	
	(0.154)	(0.161)		(0.112)	(0.151)	(0.131)	
water.temp.mean	**−0.352****	**−0.363****			**−0.376****		
	(0.108)	(0.114)			(0.114)		
water.temp.mean.lag3					0.176		
					(0.090)		
water.temp.sd	**0.502****	**0.484****			**0.441****		**0.358***
	(0.146)	(0.154)			(0.146)		(0.140)
water.temp.sd.lag1	**−0.626*****	**−0.657*****			**−0.552*****		**−0.425****
	(0.146)	(0.152)			(0.140)		(0.121)
water.temp.sd.lag3	**0.275***	**0.318***					
	(0.116)	(0.135)					
R^2	0.737	0.716	0.334	0.327	0.721	0.397	0.509
Adj. R^2	0.656	0.628	0.297	0.289	0.635	0.345	0.448
Num. obs.	35	35	39	39	35	39	37
MSE	0.484	0.503	0.663	0.666	0.498	0.640	0.597

$^{***}p < 0.001$, $^{**}p < 0.01$, $^{*}p < 0.05$

Table S4: Regression coefficents of the 7 best SRM-ranked models of the ecology of *Bulinus* spp. in a temporary pond. Legend as in S3.

	model1	model2	model3	model4	model5	model6	model7
a	**1.229****	**1.026***	**1.298****	**1.340***	2.783	3.935	1.610
	(0.361)	(0.358)	(0.371)	(0.491)	(2.453)	(4.247)	(0.734)
N_t	**−0.129*****	**−0.132*****	**−0.137*****	**−0.122*****	**−0.132*****	**−0.133*****	**−0.132*****
	(0.020)	(0.019)	(0.021)	(0.023)	(0.021)	(0.021)	(0.021)
air.temp.mean.lag3						−0.110	
						(0.173)	
air.temp.sd.lag1							−0.120
							(0.200)
precip.30		0.003					
		(0.002)					
precip.events.30			0.106				
			(0.115)				
water.temp.mean.lag1					−0.049		
					(0.076)		
water.temp.sd				**−0.501****			
				(0.157)			
water.temp.sd.lag1	**−0.616****	**−0.554****	**−0.592****		**−0.587****	**−0.514***	**−0.555***
	(0.146)	(0.141)	(0.150)		(0.157)	(0.219)	(0.182)
water.temp.sd.lag3	**0.678*****	**0.603*****	**0.596****	**0.466*****	**0.616****	**0.644*****	**0.625****
	(0.111)	(0.113)	(0.144)	(0.092)	(0.150)	(0.126)	(0.145)
R^2	0.856	0.886	0.867	0.804	0.861	0.861	0.861
Adj. R^2	0.816	0.841	0.813	0.750	0.806	0.806	0.805
Num. obs.	15	15	15	15	15	15	15
MSE	0.247	0.229	0.248	0.287	0.254	0.254	0.254

$^{***}p < 0.001$, $^{**}p < 0.01$, $^{*}p < 0.05$

Table S5: Regression coefficents of the 7 best SRM-ranked models of the ecology of *Bulinus* spp. in an ephemeral stream. Legend as in S3.

	model1	model2	model3	model4	model5	model6	model7
a	1.013	1.410	1.499	1.448	2.738	1.257	2.807
	(1.913)	(2.026)	(1.986)	(2.069)	(2.230)	(2.002)	(2.654)
L_t	**−0.911*****	**−1.045*****	**−1.036*****	**−0.939*****	**−0.993*****	**−0.900*****	**−1.060*****
	(0.137)	(0.144)	(0.141)	(0.137)	(0.147)	(0.141)	(0.150)
air.temp.mean							0.227
							(0.143)
air.temp.sd.lag3	**0.385****	**0.360****	**0.412*****	**0.300****	**0.288***	**0.386****	**0.470*****
	(0.110)	(0.102)	(0.105)	(0.097)	(0.114)	(0.114)	(0.101)
conductivity.mean.lag2	**0.068*****	**0.053*****	**0.059*****	**0.044****	**0.058*****	**0.064*****	**0.060*****
	(0.013)	(0.013)	(0.013)	(0.012)	(0.013)	(0.014)	(0.013)
conductivity.mean.lag3	**−0.039****				−0.017	−0.020	
	(0.013)				(0.012)	(0.012)	
conductivity.sd.lag3	**0.279*****	**0.250*****	**0.282*****	**0.251*****	**0.248*****	**0.271*****	**0.279*****
	(0.063)	(0.063)	(0.065)	(0.064)	(0.062)	(0.065)	(0.065)
precip.14	**0.019*****	**0.016*****	**0.017*****		**0.015*****	**0.017*****	**0.017*****
	(0.004)	(0.004)	(0.004)		(0.004)	(0.004)	(0.004)
precip.events.14				**0.599*****			
				(0.141)			
water.level.mean.lag1		**−0.006*****	**−0.006*****	**−0.006****	**−0.007*****	**−0.005****	**−0.006*****
		(0.002)	(0.002)	(0.002)	(0.002)	(0.002)	(0.002)
water.level.sd.lag1	**−0.019*****						
	(0.005)						
water.temp.mean	**−0.198*****		−0.123			**−0.222*****	**−0.528***
	(0.055)		(0.076)			(0.058)	(0.205)
water.temp.mean.lag2		**−0.225*****	−0.142	**−0.194****	**−0.225*****		
		(0.059)	(0.077)	(0.059)	(0.059)		
R^2	0.644	0.606	0.631	0.589	0.624	0.623	0.623
Adj. R^2	0.570	0.535	0.553	0.515	0.545	0.544	0.543
Num. obs.	47	47	47	47	47	47	47
MSE	0.657	0.683	0.670	0.698	0.676	0.677	0.677

$^{***}p < 0.001$, $^{**}p < 0.01$, $^{*}p < 0.05$

Table S6: Regression coefficents of the 7 best SRM-ranked models of the ecology of *Biomphalaria pfeifferi* in a perennial stream. Legend as in S3.

	model1	model2	model3	model4	model5	model6	model7	model8
a	1.178	0.105	**3.567***	1.599	1.323	0.889	0.184	2.394
	(0.948)	(0.855)	(1.492)	(0.999)	(1.008)	(0.975)	(0.404)	(1.429)
L_t	**−0.871*****	**−0.836*****	**−0.895*****	**−0.845*****	**−0.815*****	**−0.871*****	**−0.741*****	**−0.903*****
	(0.115)	(0.124)	(0.114)	(0.116)	(0.121)	(0.115)	(0.118)	(0.118)
air.temp.sd.lag2	**0.305*****		**0.222****	**0.281*****	**0.274*****	**0.300*****	**0.308*****	**0.272****
	(0.071)		(0.078)	(0.073)	(0.075)	(0.071)	(0.066)	(0.077)
air.temp.sd.lag3		**0.334*****						
		(0.067)						
conductivity.mean		**−0.019***	**−0.020***					−0.009
		(0.008)	(0.010)					(0.008)
conductivity.mean.lag3	**−0.020***		**−0.029****	**−0.020***	**−0.027****	**−0.019***		**−0.023***
	(0.009)		(0.010)	(0.009)	(0.010)	(0.009)		(0.010)
conductivity.sd			0.094					
			(0.046)					
conductivity.sd.lag1		**−0.111***						
		(0.043)						
conductivity.sd.lag3	**−0.123***		**−0.133****	**−0.149****		**−0.135****	**−0.141****	**−0.114***
	(0.049)		(0.048)	(0.052)		(0.049)	(0.052)	(0.049)
water.level.mean.lag1		**0.009*****						
		(0.002)						
water.level.mean.lag2				−0.005				
				(0.004)				
water.level.mean.lag3	**0.005****		**0.005****	**0.008****	**0.005****	**0.005****		**0.005****
	(0.002)		(0.001)	(0.003)	(0.002)	(0.002)		(0.002)
water.level.sd.lag2	**0.014****		**0.016****	**0.020****	**0.011***	**0.015****	**0.023*****	**0.015****
	(0.005)		(0.005)	(0.006)	(0.005)	(0.005)	(0.005)	(0.005)
water.temp.sd						0.248		
						(0.212)		
R^2	0.628	0.556	0.676	0.643	0.567	0.641	0.518	0.640
Adj. R^2	0.571	0.502	0.606	0.577	0.513	0.575	0.471	0.574
Num. obs.	46	47	46	46	46	46	46	46
MSE	0.541	0.577	0.519	0.537	0.577	0.539	0.601	0.539

$^{***}p < 0.001$, $^{**}p < 0.01$, $^{*}p < 0.05$

Table S7: Regression coefficents of the 8 best SRM-ranked models of the ecology of *Bulinus* spp. in a perennial stream. Legend as in S3.

Table S8: Proposition of remote-sensing data sources for upscaling hydro-ecological forecasting

Data type	Purpose	Data source	Resolution		Web
			space	time	
Water bodies	Habitat identification by extracting of water surfaces from satellite imagery	Landsat [a]	30m	16 days	http://earthexplorer.usgs.gov/
		NASA MODIS [b]	250m	8 days	https://lpdaac.usgs.gov/dataset_discovery/modis/modis_products_table/mod09q1
Evapo-transpiration	Quantification of habitat ephemerality	NASA MODIS [b]	1km	8 days	ftp://ftp.ntsg.umt.edu/pub/MODIS/NTSG_Products/MOD16/
River network	Habitat identification	Hydro-SHEDS [c]	100m	-	http://hydrosheds.cr.usgs.gov/dataavail.php
Land surface temperature	Environmental covariate for demographics modelling	NASA MODIS [b]	1km	1day	https://lpdaac.usgs.gov/dataset_discovery/modis/modis_products_table/mod11a1
Precipitation	Precipitation estimates	NASA TRMM [d]	25km	3 hours	http://gcmd.nasa.gov/records/GCMD_GES_DISC_TRMM_3B42_daily_V6.html

[a] http://landsat.usgs.gov//landsat_level_1_standard_data_products.php
[b] http://modis.gsfc.nasa.gov/data/dataprod/mod16.php
[c] [23]; Information: http://www.worldwildlife.org/hydrosheds
[d] NASA Tropical Rainfall Measurement Mission Project; [24]

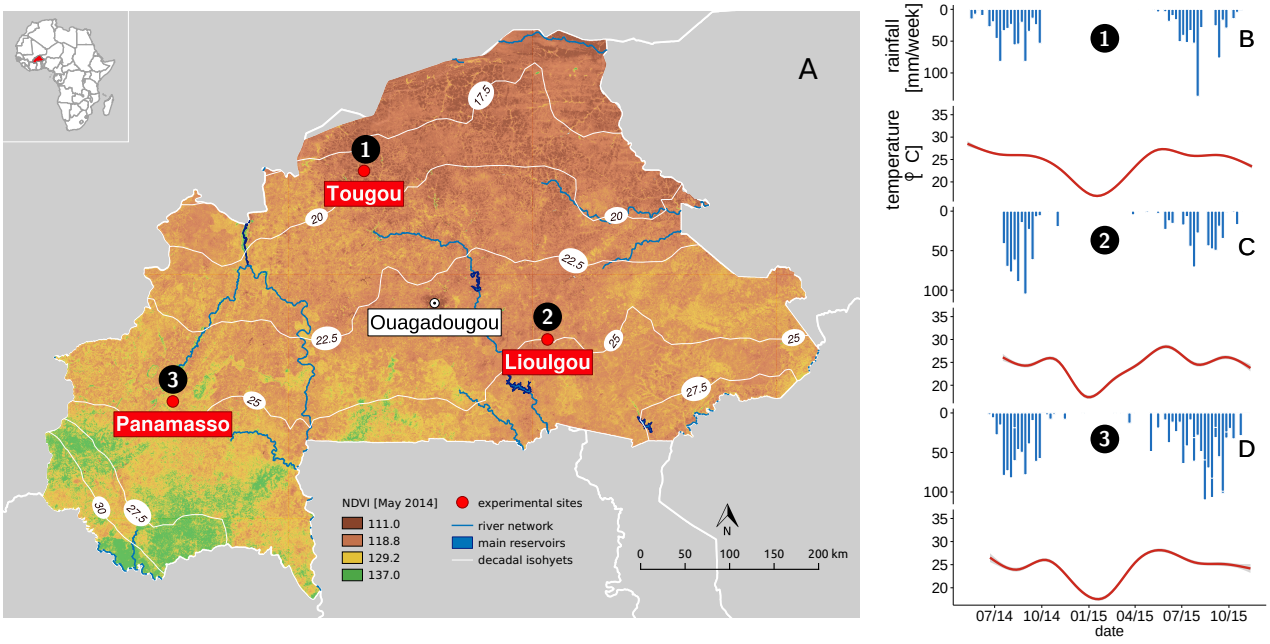

Figure S1: A: Map of the South-North climatic gradient in Burkina Faso, highlihted by values of Normalized Difference Vegetation Index and average decadal precipitation isolines. The field sites chosen for the present study are marked with red dots. The state capital, Ouagadougou, is also shown. B-D: The right panels show measured cumulative weekly precipitation (blue bars) and average daily air temperatures (red lines) in the experimental sites of Tougou (B), Lioulgou (C) and Panamasso (D). Note the different starting measurement dates in each experimental site.

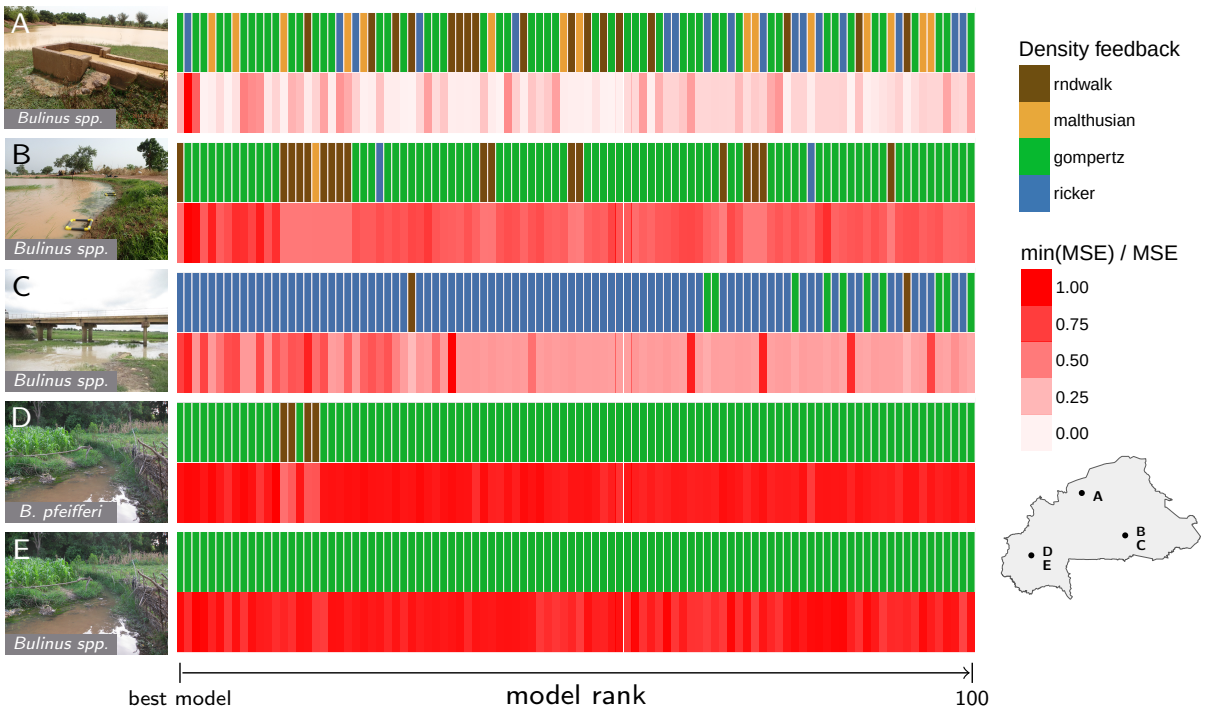

Figure S2: Density feedback detection in snail population dynamics. Model structures selected by the SRM criterion are shown by row for *Bulinus* spp. in the irrigation canal in Tougou (A), the temporary pond (B) and the ephemeral stream (C) in Lioulgou, and in the perennial stream in Panamasso (E), *B. pfeifferi* is only present in the latter (D). Each column represents a model structure, ranked in descending SRM criterion order (first from the left being the best). Density feedback is associated to model type: Malthusian (yellow) correspond to no feedback, Gompertz (green) to mild, anRicker (blue) to strong feedback, and random walk models are indicated in brown. Relative model predictive power is illustrated by the ratio of the smallest cross-validation mean squared error, $\min(\text{MSE}^{\text{cv}})$, to the model MSE^{cv}, 1 (red) indicating best relative predictive power among candidate models for a given habitat an species. The inset to the right gives the indicative location of the sampling sites in Burkina Faso.

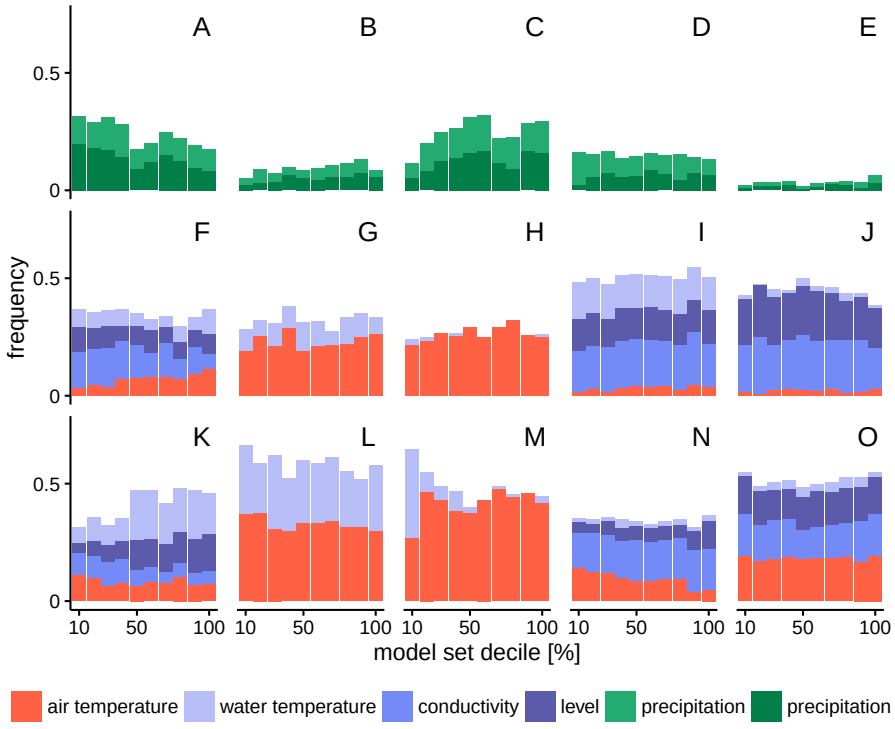

Figure S3: Environmental covariates and snail population dynamics. The importance of measured environmental covariate features is given in terms of the frequency of appearance in the 500 best selected models, summarized by decile (decile 10 corresponds to top 10% model rankings). Results are shown by columns for *Bulinus* spp. in the irrigation canal (A-K), in the temporary pond (B-L), in the ephemeral stream (C-M), and for *B. pfeifferi* (D-N) and *Bulinus* spp. (E-O) in the perennial stream. Results are partitioned by row by the type of covariate feature, including cumulative sums for precipitation (row A-E), and weekly average (F-J) and standard deviation (K-O) for air temperature and water conductivity, level and temperature.

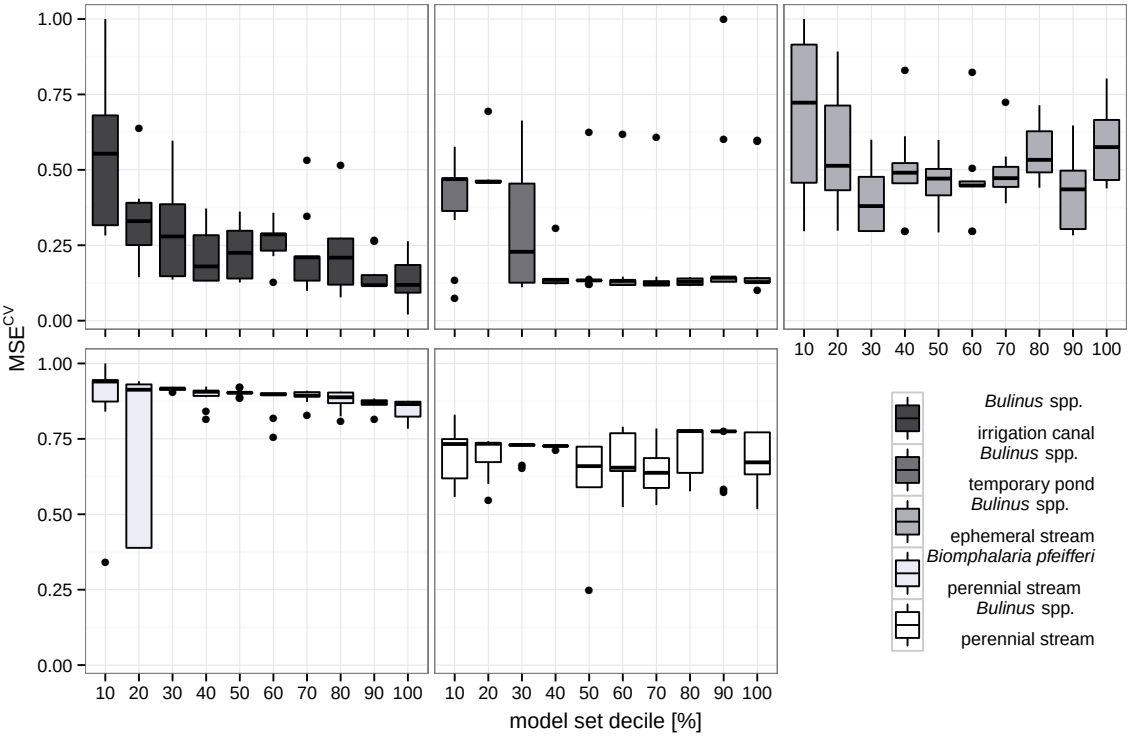

Figure S4: SRM criterion rank and predictive capacity. Cross-validation error boxplots are given for each decile for the top 100 models selected by the SRM criterion. Results are partitioned by species and habitat.

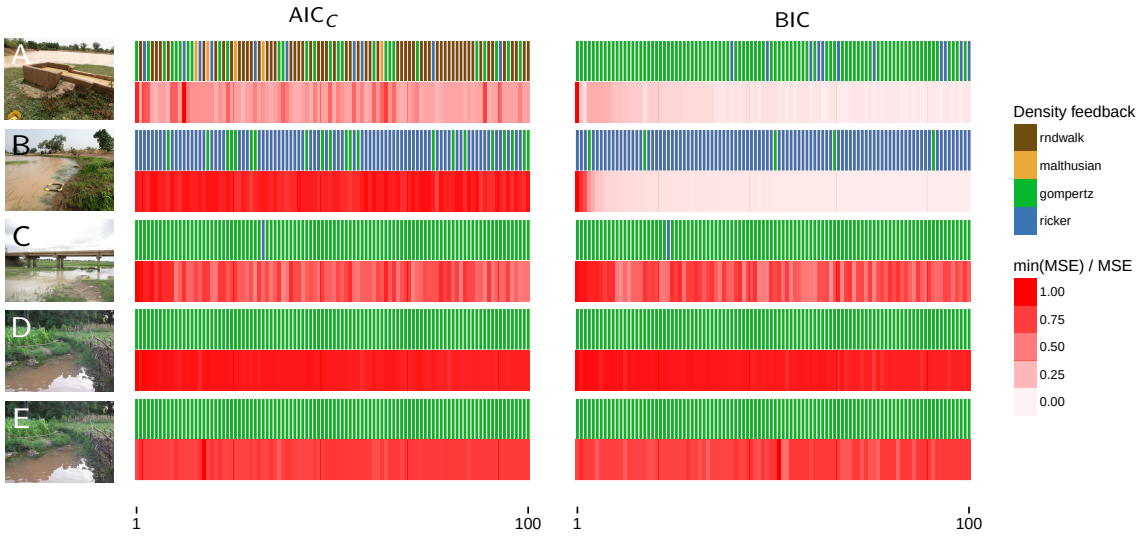

Figure S5: Model identification and cross-validation error with the AICc and BIC criteria. Results are given in the same order and using the same colorcoding as Fig. S2, for *Bulinus* spp. in the irrigation canal in Tougou (A), in the ephemeral pond (B) and stream (C) of Lioulgou, and in the perennial stream of Panamasso for *B. pfeifferi* (D) and *Bulinus* spp. (E).

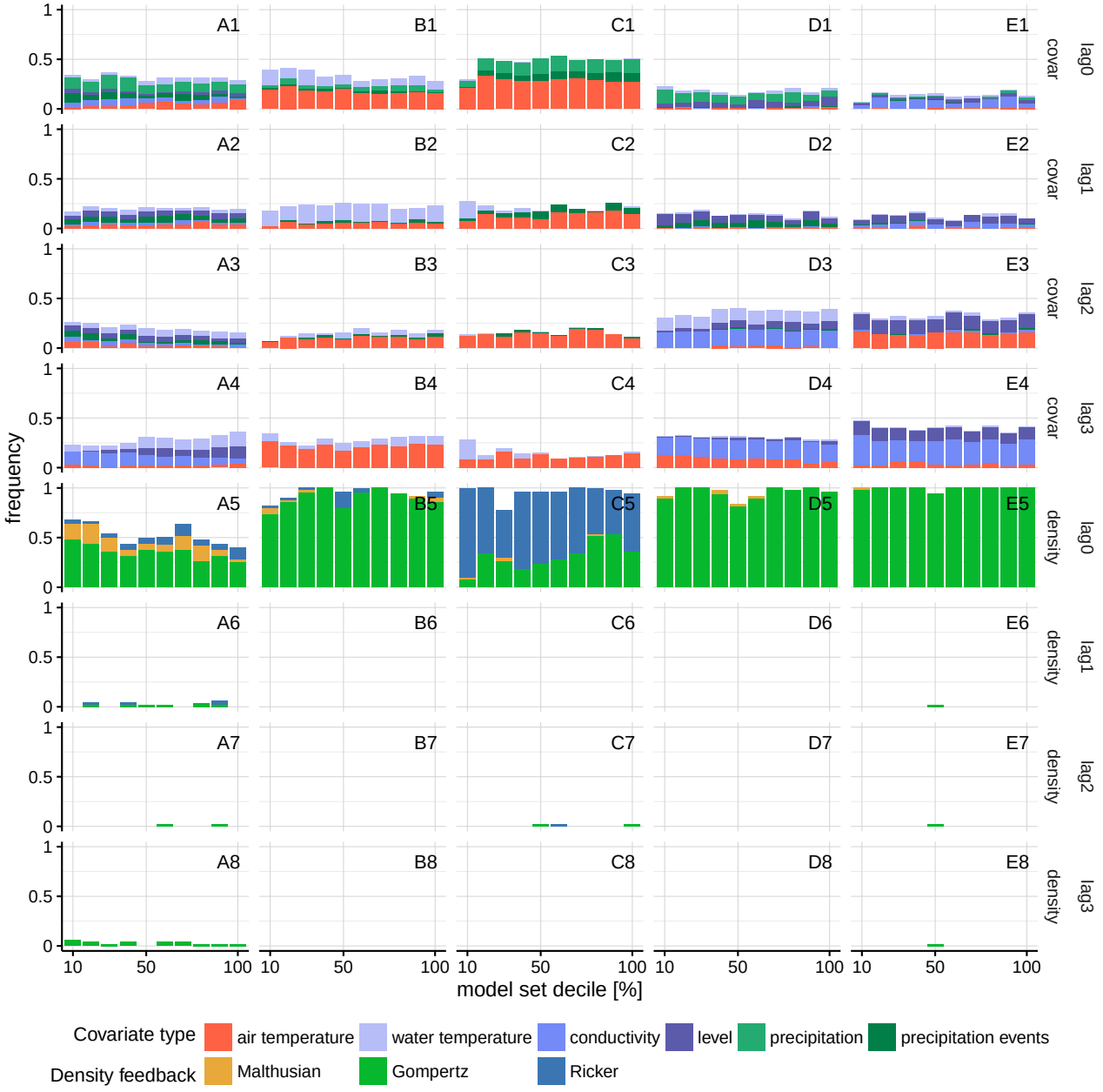

Figure S6: Lags in the effects of exogenous forcing and density dependence on snail population dynamics. Data is given by column for *Bulinus* spp. in the irrigation canal (column A), in the temporary pond (B), in the ephemeral stream (C), and for *B. pfeifferi* and *Bulinus* spp. in the perennial stream (D, E). Data is partitioned by row in terms of lags: no lag (rows 1,5), 1 week lag (2,6), 2 weeks lag (3,7) and 3 weeks lag (4,8). Note that all environmental covariates are measured during the week preceding sampling, thus meaning that the 3 week lagged value of mean water temperature corresponds to the weekly average of water temperature on 4 weeks before collection. Environmental covariates and density feedback mechanisms are given in the color legend.

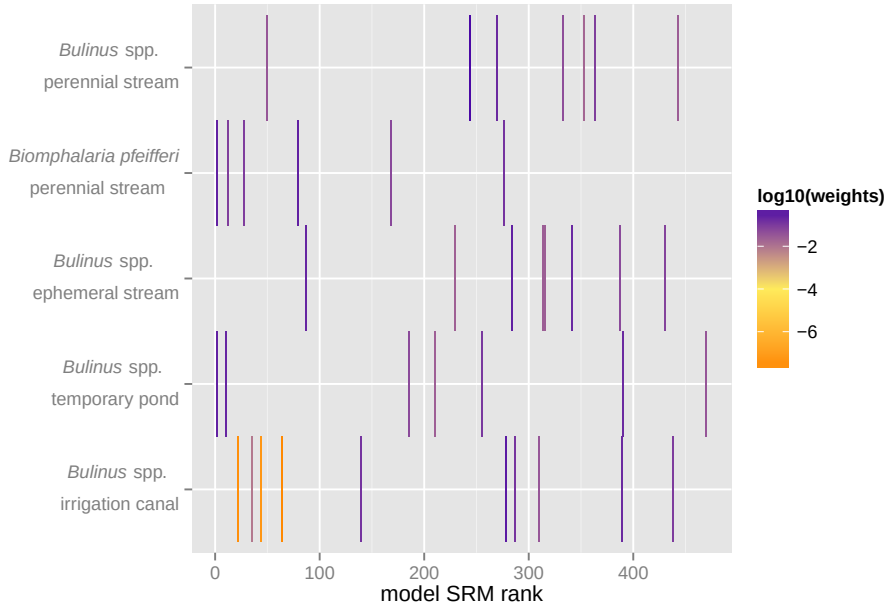

Figure S7: Jackknife model averaging weights. Model average weights are given for each species and habitat, weights sum 1 over the rows.

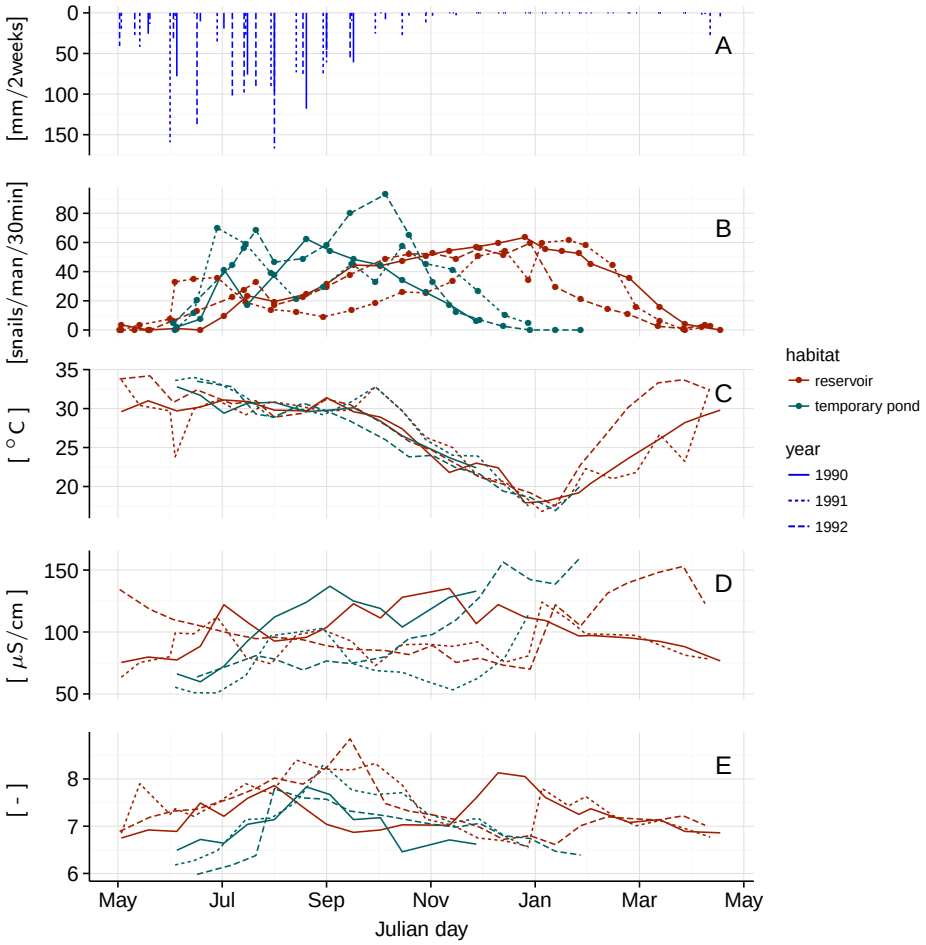

Figure S8: Historical *Bulinus* spp. abundance and covariate data in Burkina Faso. Data were collected by Poda and collaborators during three years (1990, 1991 and 1992, indicated by full, dotted and dashed lines). A) biweekly precipitation, B) *Bulinus* spp. abundance, C) water temperature, D) conductivity, and E) pH. Colours indicate data collected in a small reservoir (brown) and a temporary pond (turquoise), both located in the same area (see the Historical data section in this SI). Note that the precipitation data are the same for both habitats. The interruption of the temporary pond time-series indicate the drying of the pond. Data from [2, 25, 3].

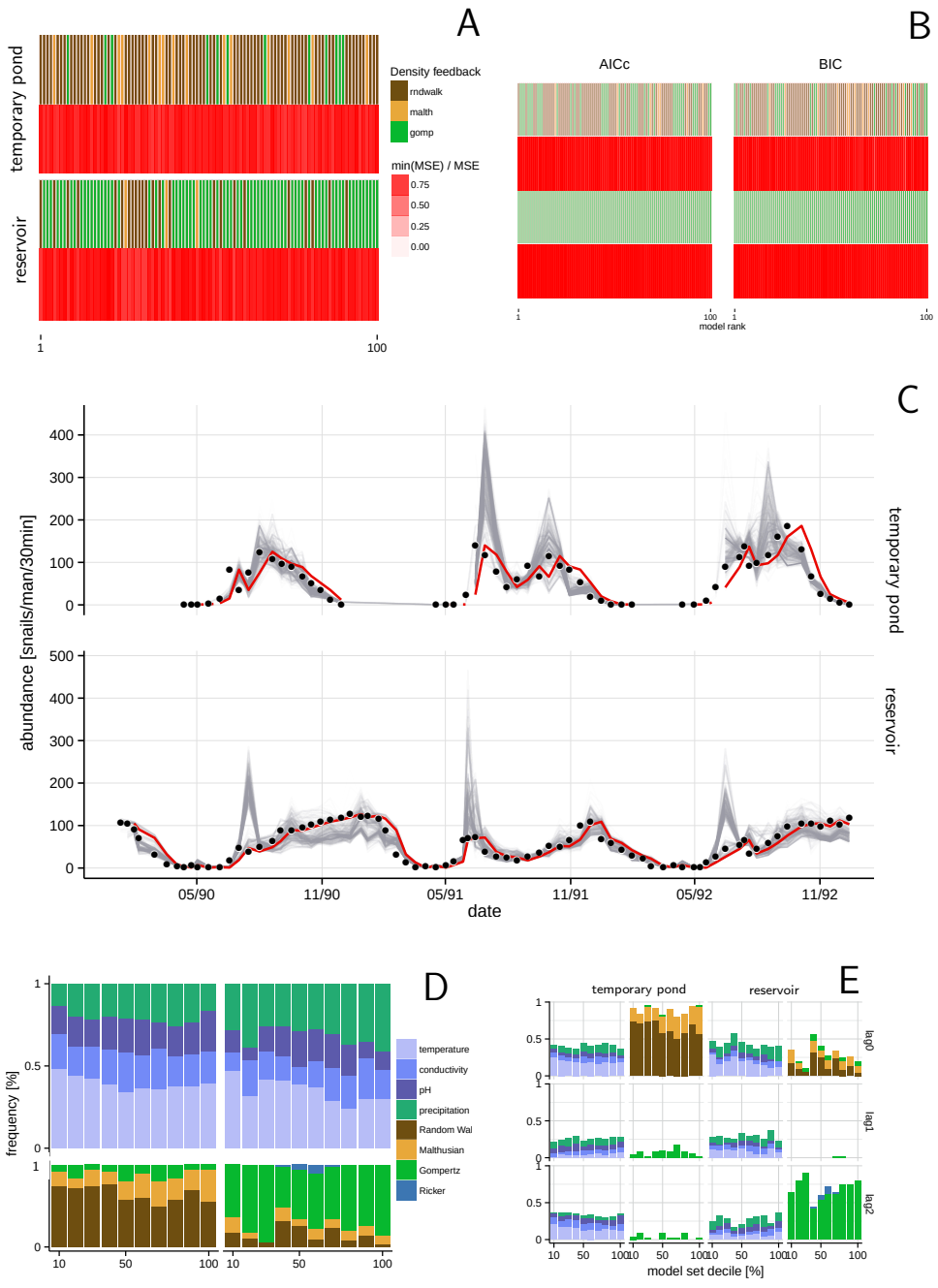

Figure S9: Ecological modeling results of historical snail sampling in Burkina Faso. Results are shown for model selection (using SRM in panel A and AICc and BIC in panel B, legend as Fig. S2), population dynamics prediction (C, legend as Fig. 3), overall covariate occurrence (D, legend as Fig. 2), and lagged covariate occurrence (E, legend as Fig. S6), for *B. senegalensis* in a temporary pond (top rows in panels A, B and C, left columns in panels D and E) and *B. truncatus* in a small reservoir (bottom rows in panels A , B and C, right columns in panels D and E). Environmental covariates correspond to the ones in Fig. S8. In panel C models with predictions larger than 350 snails/man/30min were removed for plotting purposes, all removed models were in the bottom 500 models selected by the SRM criterion.